Uma *et al.*
Protection and Control of Modern Power Systems (2023) 8:63
https://doi.org/10.1186/s41601-023-00336-4

Protection and Control of
Modern Power Systems

ORIGINAL RESEARCH **Open Access**

Adaptive overcurrent protection scheme coordination in presence of distributed generation using radial basis neural network

Uma Uzubi Uma[1*], Daniel Nmadu[1†], Nnaemeka Ugwuanyi[1†], Ogah Ekechi Ogah[1†], Ngozi Eli-Chukwu[1†], Marcellinus Eheduru[1†] and Arthur Ekwue[2†]

Abstract
The operational performance of conventional overcurrent protection relay coordination connected to a distribution network is adversely affected by the penetration of distributed generators (DG) at different buses in the network. To address this problem, this paper proposes a novel adaptive protection coordination scheme using a radial basis function neural network (RBFNN), which automatically adjusts the overcurrent relay settings, i.e., time setting multiplier (TSM) and plug setting multiplier (PSM) based on the penetration of DGs. Short circuit currents and voltages measured at different buses are acquired using the remote terminal units (RTU) connected to different buses within the terminal network. Communication between the various remotes and local end station RTUs is through hybrid communication systems of fiber optic and power line communication system modules. The new adaptive overcurrent protection scheme is applied to the IEEE 33-bus distribution network with and without DGs, for single and multi-DG penetration using both the ETAP and MATLAB software. The simulation results show the proposed scheme significantly improves the protection coordination.

Keywords Adaptive protection, Distributed generation, Overcurrent relay, Protection coordination, Radial basis function

1 Introduction

The constant increase in global warming calls for alternative energy supplies to reduce carbon emissions. This leads to the increase in the integration of different renewable energy sources (such as PV, wind, biomass, etc.) into the power network [1]. Distributed generation (DG), also called decentralized generation or embedded generation, consists of small generators or electric power sources connected directly to the distribution network. The installation of DG has many economic advantages such as reducing losses in the power system, improving voltage profile, increasing energy efficiency, improving power quality and lowering operational costs.

However, DG installation poses significant challenges to the power system network protection because of the unforeseen short circuit current increase in the distribution network [2]. Different DG loadings affect the short circuit current. This causes the setting of the conventional relay to change regularly [3]. In addition, DG penetration causes a bi-directional power flow, which often leads to a complete loss of coordination in the power system protection scheme, undesired system islanding, and maloperation of the DG protection scheme [4]. Within

† Daniel Nmadu, Nnaemeka Ugwuanyi, Ogah Ekechi Ogah, Ngozi Eli-Chukwu, Marcellinus Eheduru, Arthur Ekwue contributed equally to this work.

*Correspondence:
Uma Uzubi Uma
gbogbonna@yahoo.co.uk
[1] Department of Electrical/Electronics Engineering, Alex Ekwueme Federal University, Ndufu-Alike, Ikwo, PMB 1010, Abakaliki, Ebonyi State, Nigeria
[2] Department of Electrical Engineering, University of Nigeria, Nsukka, Enugu State, Nigeria

the last decade, many studies have been carried out into protection scheme problems in the presence of DGs and how to prevent the protection scheme loss of coordination between different conventional relays within the power system network.

In [5], an overcurrent relay coordination algorithm is presented in the presence of DG using a directional overcurrent relay to overcome the penetration effect of DG, while [6] suggests a dual setting of the directional overcurrent relay to overcome the bi-directional problem. In [7], an algorithm to solve the coordination problem by dividing the whole power system network into different zones and installing circuit breakers for different zones is presented. However, this method is faced with a limitation of the distribution network size. Reference [8] proposes the use of fault current limiters to reduce the fault contribution from different DGs connected in the network. These are a major cause of miscoordination of the power system protection relays. However, this results in power dissipation across the fault current limiters and thus increased power losses. The traditional protection systems in the presence of DGs suffer from a lack of sensitivity and slow response to a fault [9]. Reference [10] proposes a protection coordination constraint that limits the size of DG penetration in the network. However, these approaches prevent the DG from operating at its full capacity and from operating optimally.

The existing protection schemes and relay calibration can lead to inappropriate tripping when DGs are introduced to the network [11]. As the power system network evolves because of the integration of DGs, studies are ongoing to find alternative ways of solving the problem of current protection scheme coordination. An adaptive distribution protection system is therefore needed. Such a system automatically adjusts the setting of the protection system relay based on the prevailing system conditions in line with the modifications of the system operational parameters [12]. Reference [13] proposes an overcurrent protection scheme to determine the exact location of faults using a multi-layer perceptron (MLP) neural network, while [14, 15] tackle the overcurrent coordination problem using directional microprocessor-based autoreclosers. Reference [16] proposes an adaptive protection scheme with a remote-end communication facility to interact between different overcurrent relays connected in the network. However, the proposed scheme does not specify a remote end communication facility and similar to [7], does not create alternate means of communication in the event of failure of the main communication channel. In [17], an adaptive overcurrent protection scheme is proposed using two setting groups, i.e., island and grid-connected modes to mitigate the overcurrent relay coordination problem, while [18] presents an adaptive method that recalculates the relay settings online whenever there is a change in power system topology. In [19], an adaptive overcurrent protection algorithm is presented that adapts the protection system to the feeder PV penetration level concerning the changing load conditions in the distribution feeder. The algorithm analyzes sudden changes in fault current magnitude and updates the fault threshold dynamically by measuring the current magnitude at regular intervals. However, the algorithm uses the DC offset suppression capability as well as recursive least squares error to alter current phasor estimation without specifying the order of harmonics and voltage phasor. Reference [20] proposes an adaptive overcurrent protection scheme for radial distribution networks using the characteristic curve of the backup protection relay controlled by varying the location and penetration level of DGs. The backup relay characteristic curve of each relay is considered to be adaptive because it maintains the coordination time interval (CTI) between the operation of the main and backup relay within a predefined coordination region. The main advantage of this proposed scheme is that a communication medium between the network relays is not required. However, it will be difficult to implement the proposed scheme in large distribution networks with many relays because of the coordination problem (time-graded margin). An offline data adaptive protection coordination scheme based on different Setting Groups (SGs) is proposed in [21] by considering the uncertainties in distribution networks as a result of environmental factors with renewable sources. The SGs are systematically assigned to different relays based on the impedance matrix to a limit SG using the k-means method. However, the proposed algorithm did not account for relay settings outside the already set groups. Reference [22] proposes an adaptive protection system using the daily profiles of DGs and consumer forecasts to determine the day's pickup current for effective distribution coordination of the system. However, the procedure is complex and requires daily load flow analysis of the network. An intelligent online protection coordination approach is proposed in [23] where the relay settings are updated based on the DG's generation and connection mode. A similar method is used in [24] to update relay settings according to variable PV generation.

Against this background, it is important to develop an adaptive overcurrent protection scheme that responds to prevailing system conditions, namely, connection, disconnection and changing loading capacity of DGs connected to the network. This is the major cause of variation in short circuit current of the network and leads to miscoordination of the overcurrent relay protection scheme. Reference [25] presents an adaptive overcurrent coordination scheme using a differential evolution algorithm to improve the sensitivity of the backup relays. The pickup currents of different relays are recalibrated based on data output from the centralized server which performs load flow, short circuit and contingency analysis when there is a change in the system. It uses SCADA to perform its communication functions. However, the accuracy of the proposed scheme depends on the speed of the data communication and this determines the speed of decision making. In [26], an adaptive scheme is presented for a microgrid with multiple coupling points using two blocks: the offline and the online settings. The offline setting calculates the most important operating conditions of grid-connected and islanded modes, and the relay settings stored in corresponding directional overcurrent relays, while the online settings are performed based on local and global decision approaches. Reference [27] proposes two different settings for each relay with each setting selected based on the operation of a relay main or backup protection scheme. The positive sequence-based settings are selected for the main relay operation and negative sequence-based settings are chosen for the backup relay operation. However, it is complex because of the dual settings for each relay.

Reference [28] presents an improved adaptive protection scheme in the presence of DG using a centralized and decentralized communication system with two directional relays connected at remote and local ends of each feeder to isolate the faulty feeder from both sides because of DG connection. The IEC 61850 communication standard is adopted while a genetic algorithm is used to optimize the time-setting multipliers (TSM). Reference [29] presents an adaptive directional overcurrent relay protection system considering only decentralized communication systems. In [30], an adaptive protection coordination scheme of a distribution network is proposed based on the Kohonen or self-organizing map (SOM) clustering algorithm considering only inverse-time overcurrent relay characteristics. Reference [31] presents an adaptive scheme based on superimposed components of sequence currents for the protection of the microgrid. The proposed protection scheme fault current is calculated using an impact factor, obtained using pre-fault and fault currents seen by the relay. In [32], adaptive protection coordination is achieved using the current contribution calculated when the DG is connected and disconnected from the network. It is used to prevent the occurrence of protection blinding and sympathetic tripping of the protection scheme. Reference [33] proposes a scheme in distribution networks by considering the intermittency of DG using a fuzzy logic controller, in which the microcontroller selects the best TSM of the relay depending on the size of the DG connected to different buses. In [34], a scheme is proposed to address the challenges of integrating renewable energy power sources into electrical power networks by upgrading the conventional TMS in the inverse time protection setting of DOCR to a newly driven real-time adaptive variable named ATMS. The ATMS is formulated as a product of acceleration factor and turning factor. This scheme provides highly reliable protection for meshed and radial distribution networks connected to renewable energy power sources. However, the protection scheme relies on using communication systems between OCRs which is time delaying and expensive.

To address this problem, a new Radial Basis Function Neural Network (RBFNN)-based overcurrent protection scheme is proposed here. The adaptive protection scheme uses real-time short circuit current and voltage measured at the remote ends of the distribution network by the remote terminal units RTUs to adjust the overcurrent plug setting multipliers (PSM) and the TSM to attune the overcurrent protection relays to the prevailing power system distribution network conditions.

The main contributions of this paper are as follows: The penetration of distributed generations (DGs) has an impact on the calibration of TMS. In response to this, the proposed adaptive protection scheme automatically adjusts the TMS of the relays in the event of DG penetration and disconnection. The RBFNN protection model is developed considering the upper and lower limits of DG penetration, enabling maximum and minimum levels of DG integration. This scheme dynamically modifies the relay settings based on the current conditions of the distribution network, rather than relying solely on worst-case scenarios as found in existing literature. Moreover, during the islanding mode, the proposed protection scheme generates appropriate relay settings to safeguard the entire network and maintain system operation until the external grid supply is restored. The system is highly economical because it is simple to implement based on the cost of the power line communication system module and fiber optic modules embedded in normal distribution cables.

2 Design methodology

A typical IEEE 33-bus distribution network modeled in the ETAP and MATLAB software is used to illustrate the new adaptive protection scheme. The current transformers and capacitor voltage transformers connected at different buses measure the currents and voltages and other required data on the distribution network through the RTUs connected to different switchgears. The data are transmitted to the local station via a hybrid communication system (fiber optic and power line communication system) which has two different data transmission channels. The data include information on the location and presence of distributed generation, the topology of the power system, the load demand, and the performance of the protective relays in different load conditions. The data are preprocessed to remove any noise or outliers and to normalize the data to a common scale. To normalize the output signals 1 and 0, the threshold is set at 0.8, i.e., values above 0.8 are treated as 1 while values less than 0.8 are treated as 0. The value selection is based on the characteristic of the data and the desired trade-off between precision and recall in the classification task of short circuit current. The preprocessed data are trained to predict the optimal settings for the protective relays. The RBFNN is trained using a supervised feedforward backpropagation algorithm. The inputs to the RBFNN are information on the current state of the power system, such as the short circuit current, feeder location, time delay, PSM, TSM, and percentage loading of different buses. The outputs of the RBFFN are the optimal settings for the protective relays, such as the pickup current, the time delay, PSM, TSM and the feeder location. The new overcurrent relay settings are communicated to all the relays at the remote ends of the network.

2.1 Application of the radial basis function neural network (RBFNN)

The RBFNN is a type of artificial neural network that consists of three layers: an input layer, a hidden layer, and an output layer, and each layer performs specific functions in the network operation. The input layer receives the input data or features that are used to train the network. The number of neurons in this layer corresponds to the number of input variables, and each neuron represents an input variable and passes the input values forward to the hidden layer. The hidden layer of the RBFNN is responsible for transforming the input data into a nonlinear feature space. It consists of multiple neurons, where each neuron represents a radial basis function (RBF). The RBF neuron calculates the similarity between its input and a center point using a radial basis function as the activation function. The output of each hidden neuron is determined by the distance between the input data and the center point, weighted by the neuron's parameters. The output layer receives the transformed data from the hidden layer and produces the final output of the network. The number of neurons in the output layer depends on the type of problem being solved. For classification tasks, each neuron typically represents a class, and the neuron with the highest activation indicates the predicted class. In regression tasks, the output layer may consist of a single neuron that produces the predicted continuous value.

The training of the RBEFNN involves two main steps which are initialization and iterative adjustment. The RBFNN initializes the parameters of the hidden layer, including the center points and widths of the radial basis functions. These parameters can be determined using clustering algorithms, such as k-means clustering or competitive learning. The weights connecting the hidden layer to the output layer are randomly initialized, while during the training process, they are adjusted using a supervised learning algorithm, such as backpropagation. The algorithm compares the network's predicted output with the desired output and updates the weights to minimize the error. The weights of the hidden layer neurons are usually not adjusted during training.

The performance of the RBFNN depends on the proper selection of the number of hidden neurons, the centers and widths of the radial basis functions, and the appropriate training algorithm. It is often used for pattern recognition, function approximation, and time series prediction tasks because of its ability to model nonlinear relationships and capture complex patterns in data. RBFNNs have been used based on their characteristics of pattern recognition, generalization, classification of nonlinear data and ability to distinguish TSM with data falling outside the training pattern [35]. When the input partner not occupied by training data is classified, the artificial neural network (ANN) backpropagation algorithm assumes different shapes because data classification is arbitrarily done and not based on the proximity of the input data. Therefore, this algorithm lacks the required data for exact classification [36]. A RBFNN feed-forward neural network is considered a better artificial intelligence network model than the ANN especially when a radial basis function neural network with the steepest descent learning algorithm is used during the training process [37]. The RBFNN procedure as reported in [38] is adopted for the development of the proposed adaptive protection scheme.

2.2 Remote terminal unit

Within the last decade, adaptive protection schemes have attracted a lot of attention because of advances in computer and communication systems. Reference [39] states that the maximum benefit of an adaptive protection scheme can only be achieved by integrating substation control and data acquisition functions, and interfacing with the central energy management system. With the advance in technology and the development of smaller RTUs designed to be installed in substation switchgears, the adaptive protection system is fast replacing the conventional protection scheme. The Fault-Tolerant RTU (FTRTU) proposed in [40] is adopted in this work. It is important to note that the sampling time of voltage and current measurements affects the accuracy of the measurements and the performance of the overcurrent protection scheme. Therefore, it is important to carefully select the sampling time based on the specific requirements of the power system and the application of the RTU. To capture the fast-changing voltage transients, harmonics and transient current, the sampling time is set at the order of milliseconds and the sampling rate is 1 kHz.

2.3 Distributed generator sizing and location

One of the major reasons for DG placement in a distribution network is to reduce losses and increase its overall efficiency [41]. The success of DG integration lies in determining the optimal location and sizing of the DGs. In this paper, the method proposed in [42] is used to develop a MATLAB program that determines the optimal size of the DGs while the method proposed in [43] is used for the location of DG placement in the distribution network to enhance the results generated from the simulation. The total power losses in the IEEE 33-bus distribution network are calculated using the exact power loss Eq. (1) as presented in [42]. The optimal size of DG at each bus for minimizing losses is obtained using (2) and (3).

$$P_{\text{loss}} = \sum_{i=1}^{N}\sum_{j=1}^{N}\left[\alpha_{ij}\left(P_iP_j + Q_iQ_j\right) - \beta_{ij}\left(Q_iP_j - P_iQ_j\right)\right] \tag{1}$$

$$P_{\text{DG}_\text{i}} = P_{\text{D}_\text{i}} - \frac{1}{\alpha_{ii}}[\beta_{ii}Q_{\text{D}_\text{i}} + \sum_{\substack{j=1\\ j\neq i}}^{N}\left(\alpha_{ij}P_j - \beta_{ij}Q_j\right)] \tag{2}$$

$$Q_{\text{DG}_\text{i}} = Q_{\text{D}_\text{i}} + \frac{1}{\alpha_{ii}}[\beta_{ii}P_{\text{D}_\text{i}} + \sum_{\substack{j=1\\ j\neq i}}^{N}\left(\alpha_{ij}Q_j - \beta_{ij}P_j\right)] \tag{3}$$

2.4 Coordination of overcurrent relay

Relay coordination is an integral part of overall system protection and is required to isolate only the faulty circuit of the network. This can be achieved by current graded systems, time graded systems, or a combination of the two. This paper adopts an Inverse Time Definite Minimum Characteristics Relay (IDMT) for the coordination of the overcurrent relays with very inverse, extremely inverse, and standard inverse characteristics. The operation time relay can be determined according to the following procedure:

The relay current I_R is determined as:

$$I_{\text{R}} = \frac{I_{\text{f}}}{I_{\text{CT}}} \tag{4}$$

where I_{f} is the expected fault current while I_{CT} is the current transformer ratio. The relay pickup current I_{P} is calculated as:

$$I_{\text{P}} = P_{\text{setting}} \times I_{\text{SCT}} \tag{5}$$

where P_{setting} is the plug setting while I_{SCT} is the rated secondary current of CT. The PSM is calculated as:

$$PSM = \frac{I_{\text{R}}}{I_{\text{P}}} \tag{6}$$

The relay operating time is calculated as:

$$T = TSM[\frac{A}{\text{PSM}^{\infty} + \text{B}}] \tag{7}$$

where A is a constant whose value can be 0.14, 13.5, or 80, B is a constant and is equal to -1, and ∞ is a constant that varies from 0.02 to 2. K is a TSM that varies from 0.1 at an incremental step of 0.1 to 1. The following relay characteristics are used in this work, i.e.:

$$T = TSM[\frac{0.14}{\text{PSM}^{0.02} + 1}] \tag{8}$$

The protection constraints, selective and limit constraints are presented respectively as:

$$T_{\text{backup}} - T_{\text{main}} \geq CTI \tag{9}$$

$$TSM_{\text{min}} \leq TSM \leq TSM_{\text{max}} \tag{10}$$

$$I_{p\,min} \leq I_p \leq I_{p\,max} \tag{11}$$

where T_{backup} and T_{main} are the backup and main operation times of the overcurrent relay, respectively. CTI is the coordination time interval between the primary and backup relays as presented in [44]. TSM_{min} and TSM_{max}, $I_{p\,min}$ and $I_{p\,max}$ are the minimum and maximum limits of TSM and pickup current I_p, respectively. The limit constraints present in [45] are the range of relay settings from which feasible solutions are encountered and the CTI value lies between 0.2 and 0.5 s. Therefore, other constraints should be considered on the limits of relay parameters TSM and I_P.

2.5 Adaptive relay setting

The proposed relay setting model is divided into adaptive and non-adaptive modes of operation. The control system embedded in the RTU device connected to each bus monitors the activities of the DG connected to each bus and communicates its status to the central control system via the RTU for further data analysis. The control system activates the RBFNN models if the status of the DG indicates high (1), i.e., presence of DG, and deactivates RBFNN if it indicates low (0), i.e., DG penetration absent and hence, activates the initial conventional relay calibration settings of the distribution network. The network short circuit current analysis with and without DG is carried out and the procedure presented in Sect. 2.4 is used to calculate all the possible TSM required to determine the actual relay operational time. The calculated values are used to train the RBFNN models which generate different PSM, TSM, time delay, and feeder location when there is penetration of DG, and communicate the same via the RTU to the microprocessor-based overcurrent relay which updates its relay setting.

3 Simulations on power system distribution network

The case study and the protection architecture are given briefly in this section. The simulation approaches for both the conventional and the proposed adaptive schemes are then summarized.

3.1 The IEEE 33-bus distribution network model

Here the IEEE 33-bus distribution network [46] is used to model and test the proposed adaptive overcurrent protection scheme. The distribution network is modeled using the 16 software as shown in Fig. 1 while the overcurrent relay models are also implemented. The model parameters are obtained as presented in [46] and the network is divided into five different feeders. Being a radial distribution network, each feeder's protection system operates independently. Feeder 1 is made up of buses 6–18 with 12 overcurrent protection relays installed at different buses, feeder 2 spans from bus 2 through 19 to 22 with four overcurrent relays installed at different buses, feeder 3 spans from buses 3 through 23 to 25 with three overcurrent relays, and feeder 4 spans from buses 6 through 26 to 33 with eight overcurrent relays. Current transformers of rating 200/5 A are used for current measurement at 32 different buses while a capacitor voltage transformer (CVT) of 12,660/100 V is used for voltage measurement at each bus.

3.2 Adaptive overcurrent relay protection

Adaptive overcurrent protection is a protection philosophy that permits and seeks to adjust various protection functions to make them attuned to the prevailing system conditions [47]. This type of protection scheme is a feedback system and requires a communication link between the local station and the remote stations. Short circuit network analyses of line-to-ground, line-to-line, line-to-line-to-ground, and three-phase faults are carried out at each bus on the IEEE 33-bus network to generate

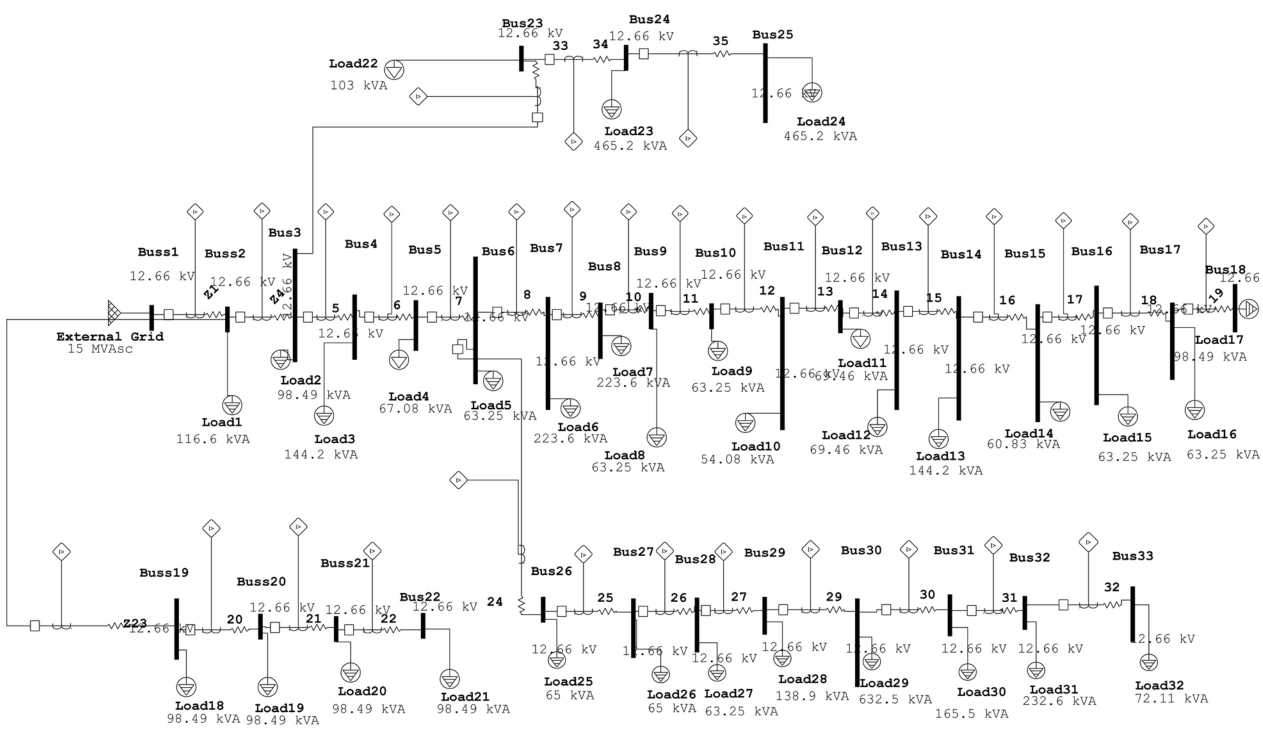

Fig. 1 The IEEE 33-bus distribution network modeled in the ETAP Software

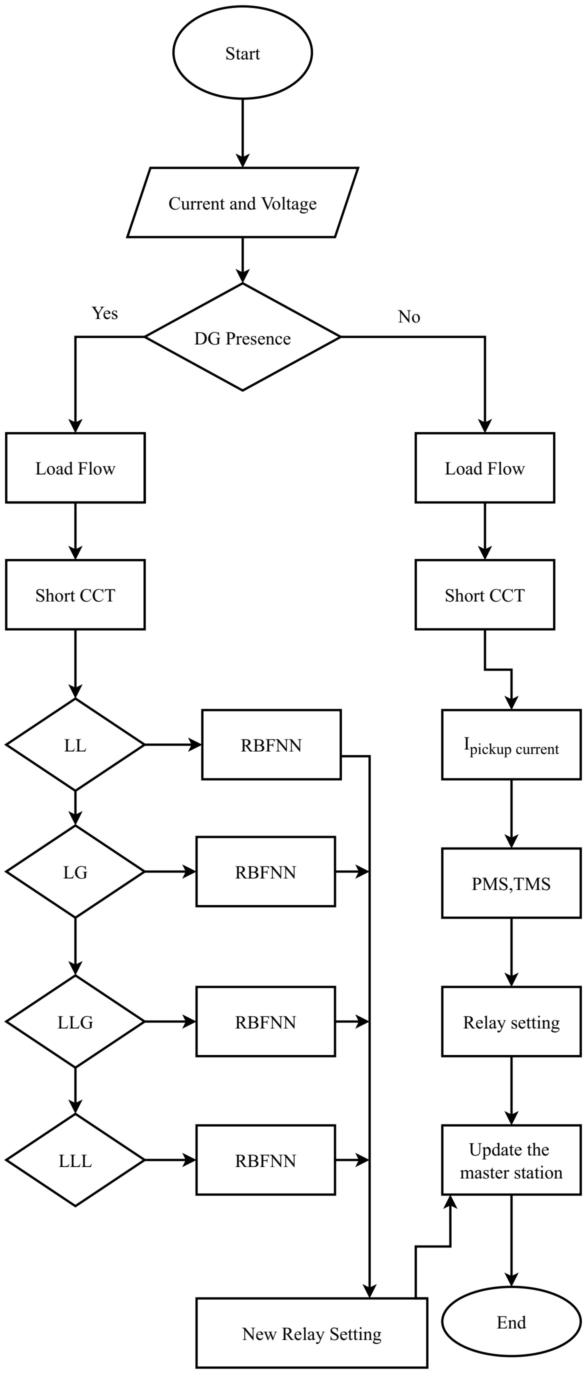

Fig. 2 Proposed adaptive overcurrent relay coordination

the required accurate data for the RBFNN training. The procedure discussed in Sect. 2.3 is used to determine the optimal size and location of DGs in the IEEE 33-bus network before DGs are introduced into the network. Short circuit analysis is equally carried out at different buses to determine the new value as a result of the DG's penetration into the network. To increase the accuracy of the results and reduce the ambiguity caused by large training data, a modular RBFNN (LG, LL, LLG, LLL) approach is adopted. The RBFNN model is divided into four different models (LG, LL, LLG, LLL) for each of the operational feeders as shown in the proposed algorithm in Fig. 2. Five different feeders are adopted with a total of twenty (20) RBFNN models for the entire distribution network. The proposed system contains a central control system which communicates with the different RTUs to determine the exact feeder that the DG is connected to or has been disconnected from. This system reduces the ambiguity involved in feeder identification, and increases the efficiency and the speed of RBFNN operation. The proposed adaptive overcurrent relay coordination protection scheme is divided into two stages. These are the protection relay coordination settings without and with DGs. Each of the stages is activated by the control system developed using the directional relays, AND gates, and OR gates connected at different buses. The RTUs connected at different remote buses communicate with the RTUs connected at the local stations via fibre optic or power line communication systems where the information is processed. Based on the network information status collected from the RTUs connected to different voltage and current transformers, the central server performs load flow and short circuit analysis. Subsequently, the different RBFNN models recalculate the new PSM and TSM of different relays and optimize the settings. The new relay settings are updated and the new PSM and TSM are sent to the microprocessor-based overcurrent relay for effective coordination of the network protection scheme.

4 Results and discussion

The IEEE 33-bus distribution system is modeled using a three-phase source of 12.66 kV, 10 MVA, and X/R ratio of 15. Load flow analyses are carried out to obtain the base case results with a total real power loss of 211 kW and reactive power loss of 143 kVar. The results obtained are the same as those presented in [48]. Please note that two different configurations are considered for this analysis, namely, coordination with and without DG penetration in the distribution network.

4.1 Simulation analysis of IEEE 33-bus without DG

Four different types of short circuit current analyses are carried out on the distribution network with and without DG penetration. The results of short circuit analysis without DG penetration are presented in Fig. 3. The colored marking with (X) indicates the opening of a breaker as presented in Fig. 4 which shows the relay sequence of operation of Feeder 1. The accurate operation must

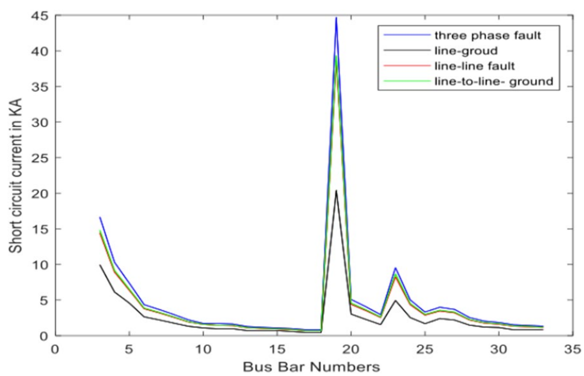

Fig. 3 Short circuit current analysis of IEEE 33-bus distribution network without DG

follow the color sequence of light green, dark green, blue, purple, gold, green, aqua and dark blue stars as the ETAP 16 software has a maximum of 9 color flashes. The short circuit current generated is used for the setting of conventional overcurrent relay protection scheme coordination, and the procedure presented in Sect. 2.4 is used for the coordination. The PSM and TSM are calculated using (4)-(7). The distribution network is divided into five different feeders.

4.1.1 Case 1 (Feeder 1)

Four different short circuit currents are introduced at bus 18. The breaker connected to bus 17 is the first to open followed by breaker connected to bus 16 to the last connected to bus 6. Figure 5 presents the time–current characteristics of the feeder 1 relay sequence of operation, and shows the simulation details (fault current, pick-up current, and actual time of operation) of each feeder relay. The vertical line represents the feeder short circuit current of 519 A, whose points of intersection with the relay characteristic curves on the y-axis represent the times corresponding to the relay characteristic curves. The feeder operational sequence follows the sequence of OR17 on the lower part as observed in Fig. 4 and increases to OR16, OR15, to OR6. This sequence shows the correct coordination of the Feeder 1 relay. The coordination time interval (CTI) between OR17 and OR16 is Δ 0.227 s, followed by Δ 0.3 s for relays between OR16 and OR15 as presented in Fig. 5. Table 1 presents the detailed simulation results as presented in Fig. 5 with OR17 operating at 176 ms with a pickup current of 1.4 A, while OR6, the last relay in the feeder, operates at 95,500 ms with a pickup current of 1.6 A. All the feeder relays are observed to have operated correctly using the specified TSM.

4.1.2 Case 2 (Feeder 2)

Different fault currents as in case 1 are introduced at bus 33 with the relay connected at bus 32 being the first to trip followed by the relay connected at bus 31 and to the last relay connected at bus 25 as presented in Fig. 6, which shows the sequence of operation with the colored marking (X) indicating the opening of the relays in descending order from breakers BK32 to BK 25. Figure 7 presents the time–current characteristics of feeder 2 which is made of 8 relays. The feeder short circuit current is represented by the vertical line which starts from point 856.1A on the x-axis. The short circuit current line intersects with all the relay characteristic curves and its points of intersection on the curve determine the times corresponding to the relay characteristic curves. Table 2 presents the relay operation sequence information. The CTI between relay 32 and relay 31 is observed as Δ 0.208 s and the CTI between relay 31 and relay 30 is observed as Δ 0.324 s which are within the standard limit of CTI as shown in Fig. 7. The accuracy of the overcurrent relay coordination of the protection feeder 2 can be observed from the characteristic curve which follows the sequence from relay 32 to relay 25. This shows accurate relay coordination because the operation successively moves from one relay to the adjacent relay. From Table 2, the first relay

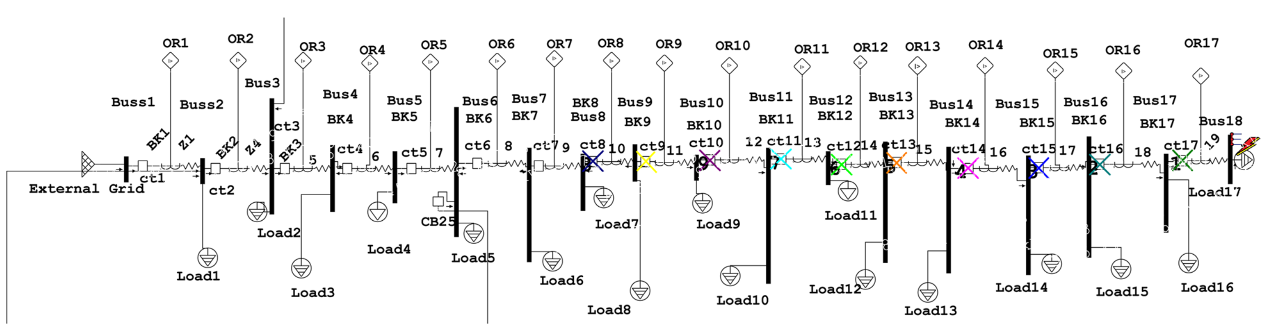

Fig. 4 Protection relay coordination of Feeder 1

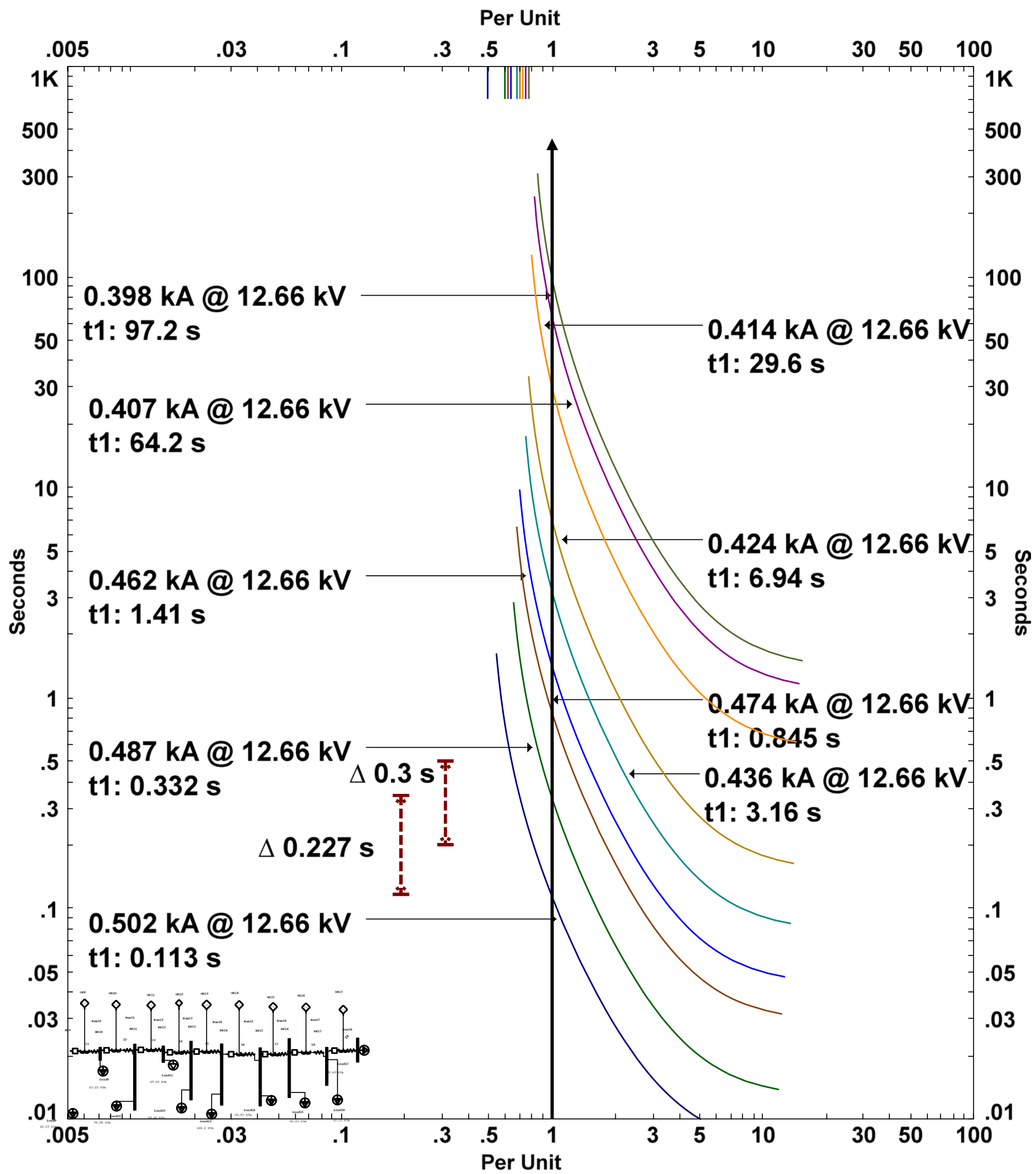

Fig. 5 Time–current characteristics of feeder 1

to operate in feeder 2 is relay 32 with a pickup current of 1.40 A and operation time of 198 ms. Relay 25 is the last to operate with a pick-up current of 1.52 A and operation time of 10,091 ms.

4.1.3 Case 3 (Feeder 3)

The same fault cases as in cases 1 and 2 are simulated for case 3 with bus 22, the faulted bus. The relay connected to bus 22 is the first to operate followed by relay connected to bus 21 while the relay connected 19 is the last one to trip as presented in Fig. 8. Figure 9 presents the time–current curve characteristics of feeder 3 which contains the simulation results of feeder 3. From Fig. 9, it is seen that the fault current is 904.4 A. The CTI between the relay 22 and 21 is calculated as Δ 0.422 s which is within the standard CTI limit while the pickup current for the relay connected to bus 22 is 2.0 A. The operational time is found to be 543 ms. The pickup current of the last relay in the feeder connected to bus 19 is found to be 2.3 A, while the relay operational time is calculated as 2,950 ms as shown in Table 3.

Table 1 Sequence of relay operation of feeder 1with conventional overcurrent protection scheme

Faulted Bus 18 without DG						Faulted Bus 18 with DG penetration		
Relay	**Time dial**	**Pickup tap**	**Short circuit current (kA)**	**Time operation (ms)**	**Operation area**	**Short circuit current (kA)**	**Time operation (ms)**	**Operation area**
OR17	0.06	2.4	0.495	176	Feeder 1	0.546	132	Maloperation
OR 16	0.07	2.450	0.479	349	Feeder 1	0.530	244	Maloperation
OR 15	0.10	2.460	0.466	557	Feeder 1	0.518	379	Maloperation
OR 14	0.19	2.470	0.454	1180	Feeder 1	0.507	778	Maloperation
OR 13	0.27	2.480	0.427	2140	Feeder 1	0.483	1296	Maloperation
OR 12	0.40	2.490	0.415	3630	Feeder 1	0.472	2091	Maloperation
OR 11	0.51	2.500	0.405	5300	Feeder 1	0.464	2878	Maloperation
OR 10	0.68	2.520	0.397	8200	Feeder 1	0.457	4189	Maloperation
OR 9	0.88	2.540	0.388	12,700	Feeder 1	0.450	5981	Maloperation
OR 8	1.14	2.560	0.380	20,000	Feeder 1	0.444	8516	Maloperation
OR 7	1.66	2.580	0.355	53,600	Feeder 1	0.425	15,204	Maloperation
OR 6	2.35	2.600	0.335	95,500	Feeder 1	0.411	25,562	Maloperation

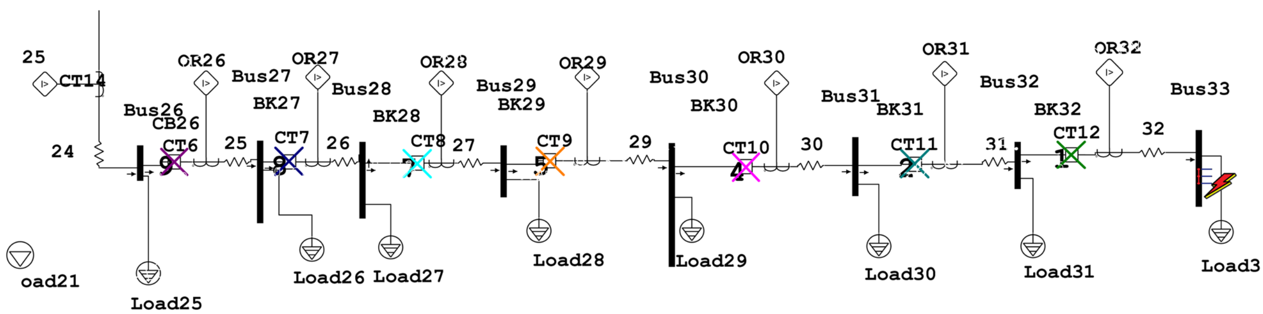

Fig. 6 Protection Relay coordination of feeder 2

4.1.4 Case 4 (Feeder 4)

The same fault cases as applied in cases 1–3 are simulated for case 4 with the faulted point being bus 25. The sequence of operations as observed in Fig. 10 shows that the relay at the far end of the feeder bus 24 trips first while the relay connected to bus 22 at the local end bus in the feeder trips last. Figure 11 presents the time–current curve characteristics with detailed information on the relay pickup current and actual time of operation. The CTI is calculated as Δ 0.203 s while the short circuit current of the feeder is found to be 1089 A. Table 4 presents the detailed simulation results of the feeder relay.

4.1.5 Case 5 (Feeder 5)

The same fault cases as applied in cases 1–4 are simulated for case 5 with the faulted point being bus 6. The relay at the far end of the feeder bus 5 (OR5) trips first while the relay (OR1) at the local end bus in the feeder trips last. The short circuit current of the feeder is found to be 1,497 A. Table 5 presents detailed simulation results of the feeder relays.

4.2 Simulation analysis of IEEE 33-bus with DG

For optimum performance of the distribution system, optimum placement and sizing analysis of the DGs are carried out to determine the accurate size of DGs required and the proper location in the distribution network since they affect the reliability of the system. The total real and reactive power required for optimum performance as presented in [49] are used for the simulation. The penetration points are buses 6 and 30. Table 1 presents the sequence of operation of feeder 1 with and without DG connection to the IEEE 33-bus distribution network. The introduction of a fault at bus 18 in the presence of DG does not follow the correct calibrated relay sequence of operation as observed in Table 5. The penetration at bus 6 and bus 30 increases the level of short circuit current across the distribution network. This causes the conventional overcurrent relay protection scheme to maloperate since its setting is based on the preset value of fault current rather than the prevailing fault.

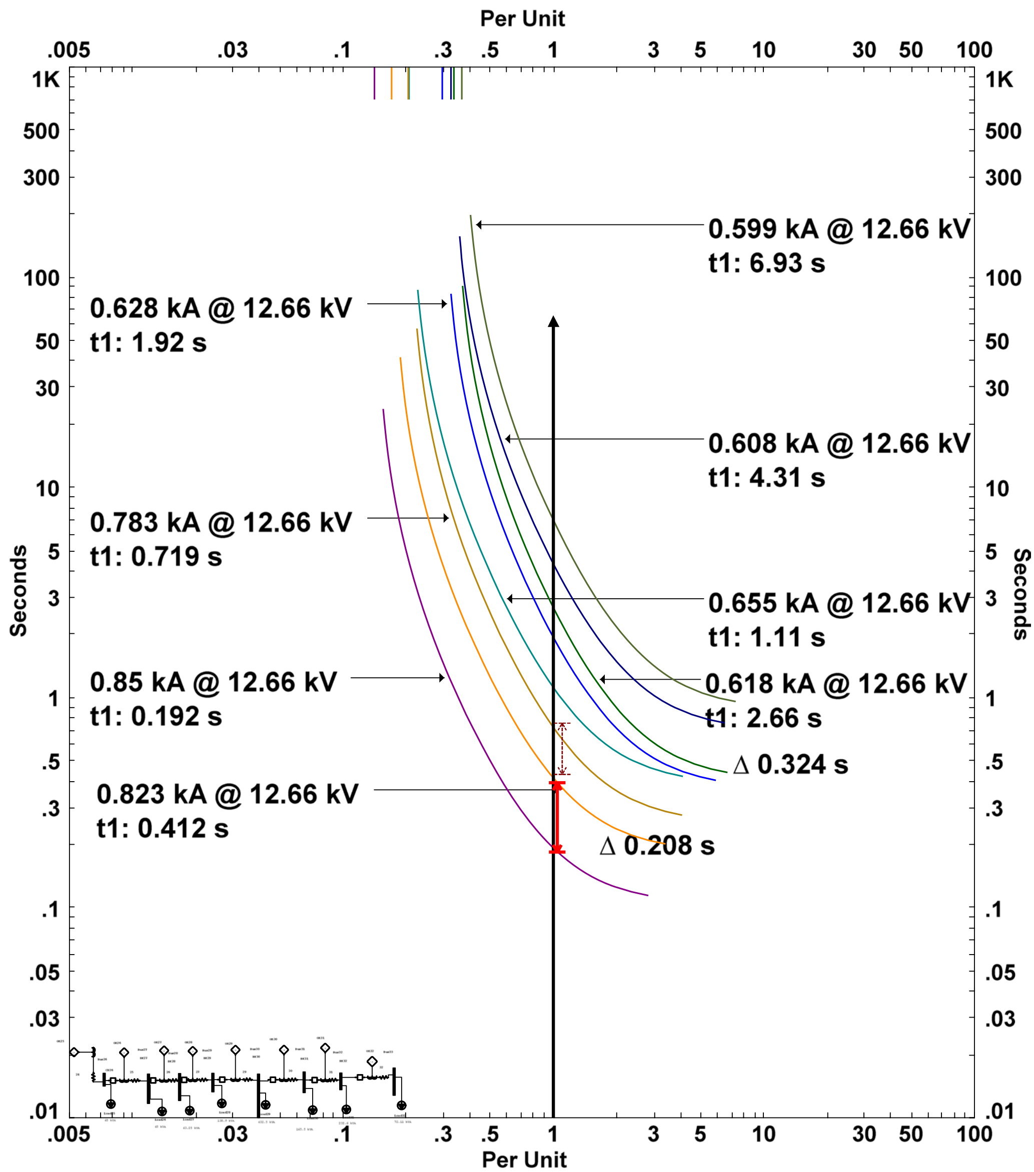

Fig. 7 Time current curve characteristics of feeder 2

4.2.1 Case 6

Fault currents are introduced in bus 18 as in case 1 and relays 17 to 6 do not operate within the specified time as observed from Table 1. The addition of DG to the distribution network increases the short circuit current from 523 to 622.1 A as observed in Fig. 12. The vertical lines represent the short circuit currents with DG at different points of DG penetration while the short line represents the short circuit current without DG. All the lines have different points of interception on the relay characteristic curve as observed from Fig. 12. The CTI between relays 17 and 16 without DG is observed as Δ 0.242 s and the CTI with DG is Δ 0.149 s. This is not within the acceptable limit. Hence, the difference is in the actual operation time of the feeder relays. The feeder relay details are equally presented in Table 1 which shows different operations when compared.

4.2.2 Case 7

Short circuit faults are introduced in bus 33 and the operation of relays 32 to 25 does not follow the specified sequence of operation. The addition of DG to the network increases the short circuit current from 856.1

Table 2 Sequence of Relay Operation of feeder 2 with conventional overcurrent protection scheme

Faulted Bus 33 without DG						Faulted Bus 33 with DG penetration		
Relay	Time dial	Pickup tap	Short circuit current (kA)	Time operation (ms)	Operation area	Short circuit current (kA)	Time operation (ms)	Operation area
OR 32	0.07	2.400	0.823	198	Feeder 2	1.159	18	Maloperation
OR 31	0.10	2.450	0.795	430	Feeder 2	1.132	29	Maloperation
OR 30	0.13	2.460	0.755	757	Feeder 2	1.095	44.4	Maloperation
OR 29	0.18	2.470	0.624	1405	Feeder 2	0.825	69.5	Maloperation
OR 28	0.19	2.480	0.596	2532	Feeder 2	0.804	117	Maloperation
OR 27	0.28	2.490	0.585	4421	Feeder 2	0.796	185	Maloperation
OR 26	0.5	2.500	0.575	6536	Feeder 2	0.790	351	Maloperation
OR 25	0.68	2.520	0.566	10,091	Feeder 2	0.784	579	Maloperation

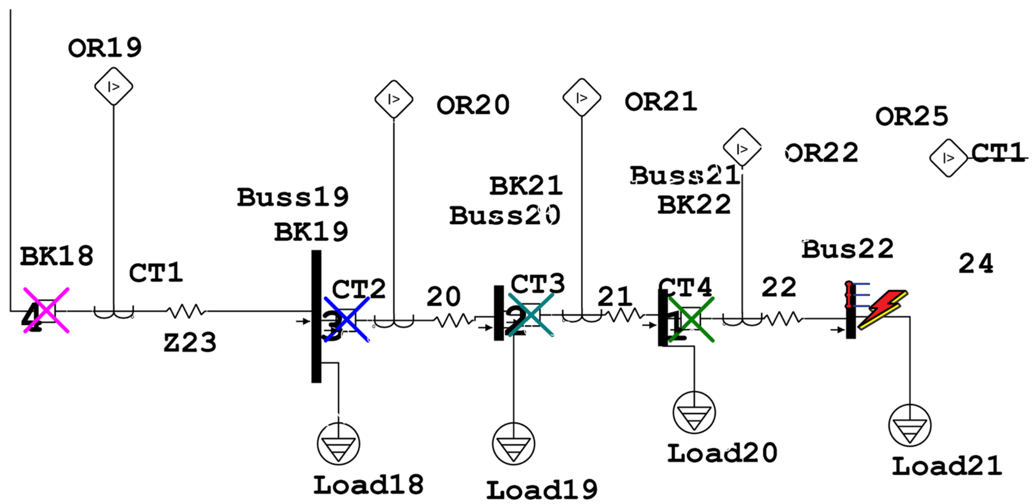

Fig. 8 Protection Relay coordination of feeder 3

to 1153 A as observed in Fig. 13. The short vertical line represents the short circuit current with DG while the other vertical lines represent the short circuit current with DG penetration at different buses. The lines meet the relay characteristic curve at different points as seen in Fig. 13. The CTI between relays 33 and 32 without DG is Δ 0.208 s and the CTI with DG is Δ 0.146 s. This is not within the acceptable limit. The difference is in the actual operation time of the feeder relays. The detailed results are presented in Table 2 which shows different operations when compared. The results of the preceding analysis clearly show that DG penetration has an impact on protection coordination. Tables 1, 2, 3, 4 and 5 demonstrate that when a DG is present in the distribution network, the short circuit level changes and the period of relay operation is incorrectly regulated, resulting in relay failure. The inability of the conventional protection scheme to modify the TSM results in a substantial discrepancy between the timings of the relay when DG is connected and disengaged is demonstrated. The following subsection will show that, with the new adaptative scheme proposed in this paper, the TSM adjusts with the system variation thereby addressing the coordination issue.

4.3 Adaptive overcurrent relay protection coordination

The RBFNN for the adaptive overcurrent protection scheme is implemented in MATLAB. The IEEE 33-bus distribution network short circuit current training data is generated using the ETAP software by introducing faults at different buses, including line-to-line, line-to-ground, line-to-line-to-ground, and three-phase faults at all the buses. A total of 512 short-circuit fault currents are generated for the training of the RBFNN model of the relay protection system. The training data are used to train the

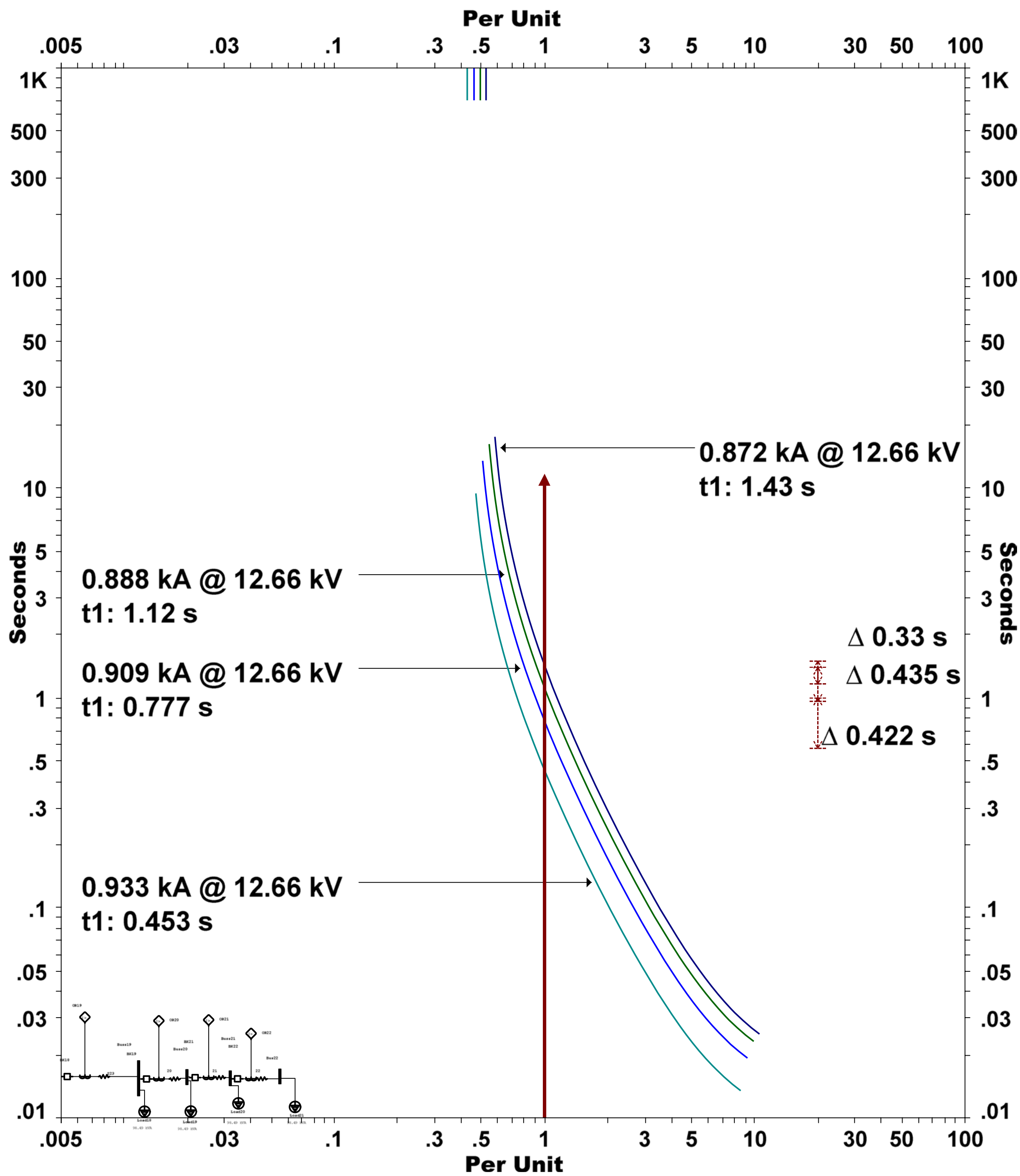

Fig. 9 Time current curve characteristics of feeder 3

Table 3 Sequence of relay operation of feeder 3 with conventional overcurrent protection scheme

Faulted Bus 22 without DG						Faulted Bus 22 with DG penetration		
Relay	Time dial	Pickup tap	Short circuit current (kA)	Time operation (ms)	Operation area	Short circuit current (kA)	Time operation (ms)	Operation area
OR 22	0.07	2.00	0.864	548	Feeder 3	1.053	342	Maloperation
OR 21	0.10	2.100	0.840	953	Feeder 3	1.031	573	Maloperation
OR 20	0.14	2.200	0.817	1630	Feeder 3	1.012	938	Maloperation
OR 19	0.21	2.300	0.800	2950	Feeder 3	0.998	1620	Maloperation

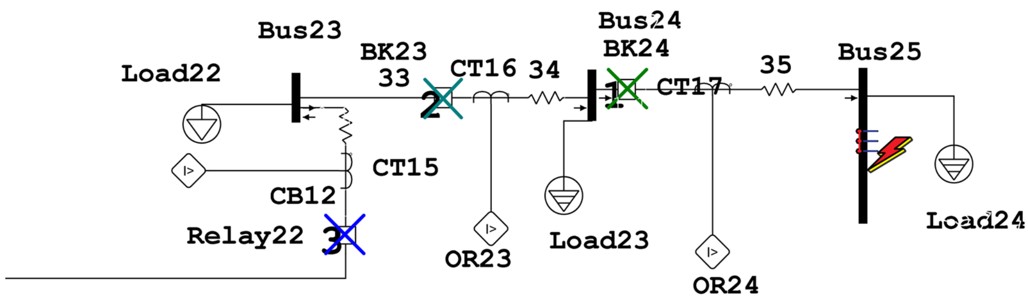

Fig. 10 Protection relay coordination of feeder 4

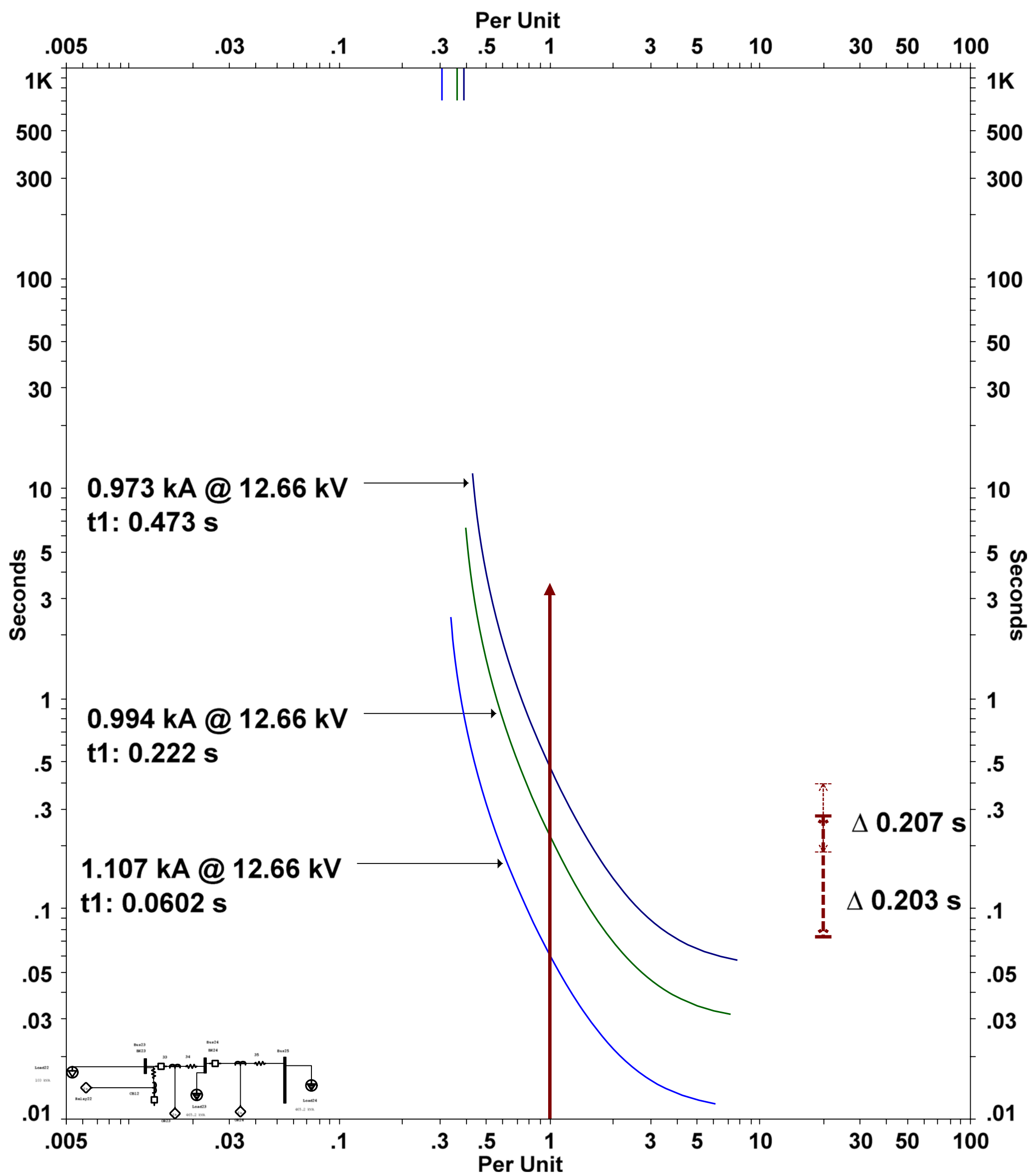

Fig. 11 Time current curve characteristics of feeder 4

Table 4 Sequence of relay operation of feeder 4 with conventional overcurrent protection scheme

Faulted Bus 24 without DG						Faulted Bus 24 with DG penetration		
Relay	**Time dial**	**Pickup tap**	**Short circuit current (kA)**	**Time operation (ms)**	**Operation area**	**Short circuit current (kA)**	**Time operation (ms)**	**Operation area**
OR 24	0.11	2.230	1.011	131	Feeder 4	1.351	77.7	Maloperation
OR 23	0.16	2.280	0.897	277	Feeder 4	1.250	143	Maloperation
OR 22	0.29	2.465	0.874	601	Feeder 4	1.232	293	Maloperation

Table 5 Sequence of relay operation of feeder 5 with conventional overcurrent protection scheme

Faulted Bus 6 without DG						Faulted Bus 6 with DG penetration		
Relay	**Time dial**	**Pickup tap**	**Short circuit current (kA)**	**Time operation (ms)**	**Operation area**	**Short circuit current (kA)**	**Time operation (ms)**	**Operation area**
OR5	0.07	2.620	0.817	118	Feeder 5	0.817	118	Maloperates
OR 4	0.18	2.640	0.800	327	Feeder 5	0.800	327	Maloperates
OR3	0.51	2.660	0.763	1060	Feeder 5	0.763	1060	Maloperates
OR2	0.48	2.680	0.496	3502	Feeder 5	0.496	3502	Maloperates
OR1	0.59	2.700	0.374	25,262	Feeder 5	0.374	25,262	Maloperates

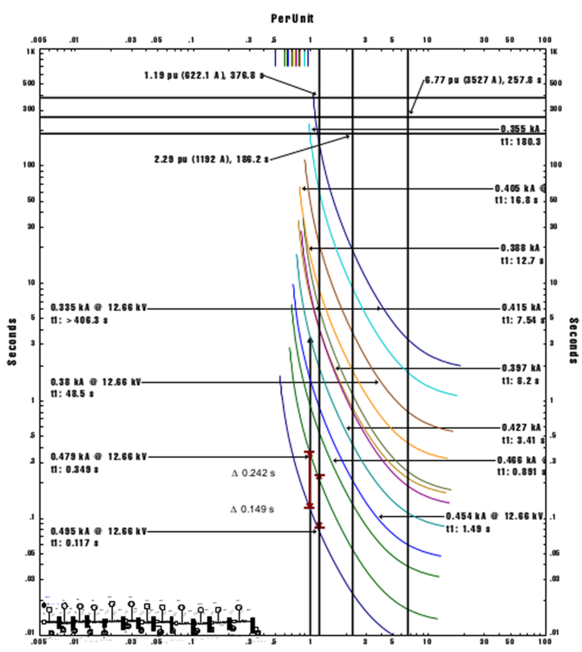

Fig. 12 Time current curve characteristics of feeder 1 with and without DG

RBFNN, i.e., to adjust the network's weights and biases to minimize the error in approximating the desired output. The training data adopted are the supervised learning format. The input layer of the RBFNN corresponds to the number of input features in the dataset, while each input feature represents the short circuit current and the current type. The output layer of the RBFNN corresponds to the number of output variables to be predicted by the network. These are the actual time of relay operation, pickup current and the time multiplier settings. After the RBFNN is trained, a new set of unseen data are evaluated to assess its generalization performance. This unseen data are referred to as the test data, which should be separated from the training data to ensure that the network performance is not biased by the data it has already seen during training. The two different DGs are loaded at their maximum and minimum operating capacities to accommodate variations in short circuit current as a result of load variation. To normalize the output of the RBFNN protection scheme trip signals 0 and 1, the threshold is set at 0.8, as previously described. This value is selected based on the validation of testing of different values and 0.8 gives the best sensitivity since protection equipment

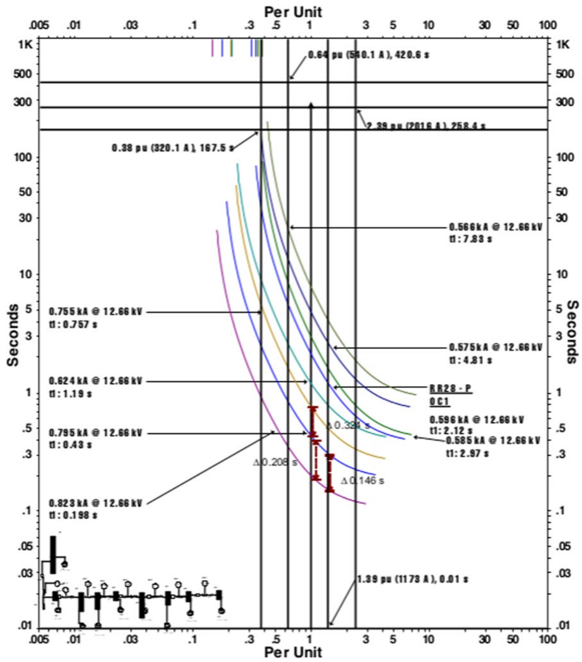

Fig. 13 Time current curve characteristics of feeder 2 with and without DG

requires a high level of precision. Each relay address is represented by a binary code for easy relay identification between the remote relays and the RBFNN master station. To reduce the complex nature of the entire protection system, a microprocessor-based directional relay is integrated into each bus to determine the on and off state of the DGs connected to different buses. A total of thirty-two (32) RBFNN models are thus developed and divided into two groups of sixteen. The two groups are protection schemes without and with DG connected to the distribution system. The CT ratio used for the adaptive protection scheme is 200/5 A, and the relay characteristic used is the standard inverse with a TSM of 1 as presented in (8). The RBFNN is configured using the following parameters: mean square error (MSE) of 0.0001, spread radial basis function of 50 and number of neurons of 100.

4.3.1 Feeder 1 adaptive setting of RBFNN relay model

A total of 204 short-circuit currents are used to develop this model. The RBFNN feeder 1 overcurrent relay model is made up of eight different RBFNN models, two each for the different types of fault current generated with and without DG. The RBFNN model achieves an MSE of 1.67188e-05 after 15 epochs as seen in Fig. 14. Table 6 presents the RBFNN overcurrent relay model setting of feeder 1 with and without DG penetration. The output of the model is TSM and PSM. The values in Table 6 are implemented in the ETAP software and the correct sequence of operation is achieved. Table 6 presents the relay calibration with and without DG penetration in the distribution network. The TSM presented when compared shows a significant difference while the actual relay operation time remains constant. This shows that TMS is the main parameter requiring adjustment to ensure that the relay operation is in tune with the prevailing network conditions. It equally shows the adaptive nature of the proposed RBFNN model towards mitigating the effect of variation of short circuit current caused by DG parameter variation. The relay operational time of the different feeders remained constant throughout the simulation. The percentage difference in the calculated TSM as presented is the major cause of the overcurrent relay coordination problem.

4.3.2 Feeder 3 adaptive RBFNN relay model with and without DG

A total of 24 short-circuit currents are generated and used for the RBFNN relay overcurrent model. The developed model without DG achieves an MSE of 8.55969e-35 after 2 epochs, and 9.45555e-45 with DG after 3 epochs. The combined results are presented in Table 7 with the PSM and the actual time of operation remaining the same. The TSM settings with and without DG penetration are not the same as observed from Table 7. The newly developed settings are implemented in the ETAP software. A short circuit fault is introduced at bus 22 and the correct sequence of relay operation is achieved. The simulation results presented in Table 7 show that the main parameter for accurate relay coordination is the TSM. The relay operational time of the different feeders remained constant throughout the simulation with or without DG, because of the new adaptive scheme which varies the TSM. The percentage differences in TSM calculated as presented in Tables 1 and 7 are the major cause of the overcurrent relay coordination problem. The adaptive model developed in this paper uses the RBFNN to generate the TSM required based on the prevailing short circuit current of the distribution network.

4.4 Comparative analysis

The performance analyses of the conventional and the proposed adaptive scheme are carried out using Tables 1, 2, 3, 4 and 5. It can be seen that penetration of DGs increases the short circuit current and thus affects the point of interception on the characteristic curve and the actual time operation of the relay. This is caused by the change in the TSM of the relay. From Tables 1 and 6, it is seen that the change in TSM of the proposed adaptive scheme is significant and ensures that the relay operation time remains constant with and without DG.

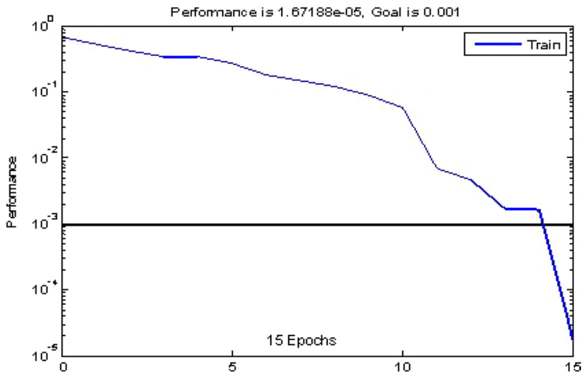

Fig. 14 Input training data for RBFNN model

5 Conclusion

This paper has described the operational performance of the adaptive overcurrent relay protection scheme of a distribution network in the presence of DG. The proposed overcurrent protection scheme generates Time Setting Multipliers (TSMs) based on the prevailing network conditions (short circuit current) rather than the preset values. The RTU constantly monitors the buses for infeed and outfeed currents, and sends the information to the local station RTU, while the proposed RBFNN model retrains the network each time their infeed current from the DGs is connected to the buses and when a DG is disconnected. The newly generated TSM is communicated to all the microprocessor-based relays connected to the network using the binary code address as output by the RBFNN. The obtained difference in TSM and the comparative TSM analysis show the adaptive nature of the RBFNN model and its accurate operational time, despite the penetration and disconnection of DGs affecting the short circuit current. The results of the proposed adaptive overcurrent protection scheme with and without DG show a more reliable and secure overcurrent distribution protection scheme than the conventional method.

Table 6 Adaptive setting of RBFNN feeder 1 with and without DG penetration

Relay	Plug setting	TSM LG With DG (Xd)	TSM LG Without DG (Yg)	Time of operation LG	TSM LLG With DG (Yd)	TSM LLG Without DG (Xg)	Time of operation LLG	% TSM LG (Xd-Yg/Yg)*100	% TSM LLG (Yd-Xg/Xg)*100
OR17	5.00	0.0247	0.0216	0.26	0.0355	0.033	0.26	14.351	7.5758
OR16	5.25	0.0404	0.0352	0.36	0.0630	0.058	0.41	14.772	8.6207
OR15	5.50	0.0539	0.0470	0.46	0.0888	0.082	0.56	14.680	8.2927
OR14	5.75	0.0684	0.0591	0.56	0.1157	0.106	0.71	15.736	9.1509
OR13	6.00	0.0854	0.0734	0.66	0.1463	0.134	0.86	16.348	9.1791
OR12	6.25	0.1189	0.1018	0.76	0.1992	0.181	1.01	16.797	10.0552
OR11	6.50	0.1361	0.1159	0.86	0.2306	0.210	1.16	17.428	9.8095
OR10	6.75	0.1505	0.1274	0.96	0.2583	0.234	1.31	18.131	10.3846
OR9	7.00	0.1949	0.1642	1.06	0.3231	0.292	1.46	18.696	10.6507
OR8	7.25	0.2759	0.2299	1.26	0.4069	0.364	1.61	20.008	11.7857
OR7	7.50	0.4278	0.3444	1.36	0.5943	0.523	1.76	24.216	13.6329
OR6	7.75	0.5310	0.4026	1.46	0.7237	0.612	1.91	31.892	18.2516

Table 7 Adaptive setting of RBFNN Zone 3 model with DG and without DG penetration

Relay	Plug Setting	TSM Without DG LG (Yg)	TSM Without DG LLG (Xg)	TSM With DG LG (Xd)	TSM With DG LLG (Yd)	Time of operation	% TSM LG (Xd-Yg/Yg)*100	% TSM LLG (Yd-Xg/Xg)*100
OR 22	5.20	0.0706	0.081	0.0708	0.0819	0.26	0.0028	1.11
OR 21	5.25	0.1127	0.128	0.1128	0.1284	0.36	0.0089	0.3125
OR 20	5.50	0.1561	0.176	0.1562	0.1766	0.46	0.064	0.340
OR 19	5.72	0.3477	0.365	0.3486	0.3715	0.56	0.258	1.780

Abbreviations

DG	Distributed generator
RBFNN	Radial basis function neural network
TSM	Time setting multiplier
PSM	Plug setting multiplier
CT	Current transformer
CVT	Capacitor voltage transformer
RTU	Remote terminal unit
PV	Photovoltaic
MLP	Multi-layer perceptron
DC	Direct current
CTI	Coordination time interval
SCADA	Supervisory control and data acquisition
SOM	Self organising map
OR/OCR	Overcurrent relay
DOCR	Directional overcurrent relay
ANN	Artificial neural network
FTRTU	Fault tolerant remote terminal unit
IDMT	Inverse time definite minimum characteristics relay
MSE	Minimum square error
SG	Setting group

Acknowledgements
Not applicable.

Author contributions
The authors contributed equally to the work.

Funding
Not applicable.

Availability of data and materials
The datasets used and/or analysed during the current study are available from the corresponding author on reasonable request.

Declarations

Competing interests
The authors declare that they have no known competing financial interests or personal relationships that could have appeared to influence the work reported in this article.

Received: 5 November 2022 Accepted: 17 November 2023
Published online: 14 December 2023

References

1. Sarangi, S., Sahu, B., & Rout, P. (2020). Distributed generation hybrid AC/DC microgrid protection: A critical review on issues, strategies, and future directions. *International Journal of Energy Research, 44*(5), 3347–3364.
2. Conti, S. (2009). Analysis of distribution network protection issues in presence of dispersed generation. *Electric Power Systems Research, 79*(1), 49–56.
3. Ustun, T., Ozansoy, C., & Ustun, A. (2012). Fault current coefficient and time delay assignment for microgrid protection system with central protection unit. *IEEE Transactions on Power Systems, 28*(2), 598–606.
4. Gopalan, S., Sreeram, V., & Iu, H. (2014). A review of coordination strategies and protection schemes for microgrids. *Renewable and Sustainable Energy Reviews, 32*, 222–228.
5. Yang, H., Wen, F., & Ledwich, G. (2013). Optimal coordination of overcurrent relays in distribution systems with distributed generators based on differential evolution algorithm. *International Transactions on Electrical Energy Systems, 23*(1), 1–12.
6. Razavi, S., Rahimi, E., Javadi, M., Nezhad, A., Lotfi, M., Shafie-Khah, M., & Catalao, J. (2019). Impact of distributed generation on protection and voltage regulation of distribution systems: A review. *Renewable and Sustainable Energy Reviews, 105*, 157–167.
7. Brahma, S., & Girgis, A. (2004). Development of adaptive protection scheme for distribution systems with high penetration of distributed generation. *IEEE Transactions on Power Delivery, 19*(1), 56–63.
8. Aslinezhad, M., Sadeghzadeh, S., & Olamaei, J. (2011). Over current relays protective coordination in distribution systems in presence of distributed generation. *International Journal on Technical and Physical Problems of Engineering, 3*(7), 40–46.
9. Shah, K., Detjen, E., & Phadke, A. (1988). Feasibility of adaptive distribution protection system using computer overcurrent relaying concept. *IEEE Transactions on Industry Applications, 24*(5), 792–797.
10. Zhan, H., Wang, C., Wang, Y., Yang, X., Zhang, X., Wu, C., & Chen, Y. (2015). Relay protection coordination integrated optimal placement and sizing of distributed generation sources in distribution networks. *IEEE Transactions on Smart Grid, 7*(1), 55–65.
11. Tushar, W., Chai, B., Yuen, C., Smith, D., Wood, K. L., Yang, Z., & Poor, H. (2014). Three-party energy management with distributed energy resources in smart grid. *IEEE Transactions on Industrial Electronics, 62*(4), 2487–2498.
12. Uma, U., Ekwue, A., & Ejiogu, E. (2020). Adaptive distance relaying: Solution to challenges of conventional protection schemes in the presence of remote infeeds. *International Transactions on Electrical Energy Systems, 30*(5), 12330.
13. Javadian, S., Haghifam, M.-R., & Rezaei, N. (2009). A fault location and protection scheme for distribution systems in presence of dg using MLP neural networks. In *2009 IEEE power & energy society general meeting* (pp. 1–8).
14. Brahma, S., & Girgis, A. (2002). *Microprocessor-based reclosing to coordinate fuse and recloser in a system with high penetration of distributed generation*. IEEE.
15. Baran, M., & El-Markabi, I. (2004). Adaptive over current protection for distribution feeders with distributed generators. In *IEEE PES power systems conference and exposition, 2004* (pp. 715–719).
16. Oudalov, A., & Fidigatti, A. (2009). Adaptive network protection in microgrids. *International Journal of Distributed Energy Resources, 5*(3), 201–226.
17. Mahat, P., Chen, Z., Bak-Jensen, B., & Bak, C. (2011). A simple adaptive overcurrent protection of distribution systems with distributed generation. *IEEE Transactions on Smart Grid, 2*(3), 428–437.
18. Amoda, O., & Schulz, N. (2007). An adaptive protection scheme for shipboard power systems. In *2007 IEEE electric ship technologies symposium* (pp. 225–230).
19. Kavi, M., Mishra, Y., & Vilathgamuwa, M. (2017). Morphological fault detector for adaptive overcurrent protection in distribution networks with increasing photovoltaic penetration. *IEEE Transactions on Sustainable Energy, 9*(3), 1021–1029.
20. Bisheh, H., Fani, B., & Shahgholian, G. (2021). A novel adaptive protection coordination scheme for radial distribution networks in the presence of distributed generation. *International Transactions on Electrical Energy Systems, 31*(3), 12779.
21. Abbasi, A., Karegar, H. K., & Aghdam, T. S. (2019). Optimal adaptive protection using setting groups allocation based on impedance matrix. In *2020 14th International conference on protection and automation of power systems IPAPS* (pp. 77–82).
22. Wahyudi, C. A. D., Hariyanto, N., & Ganjavi, R. (2019). Adaptive protection of distribution systems with DERs considering consumer and generation profiles. In *2019 International conference on smart energy systems and technologies SEST* (pp. 1–6).
23. Xu, K., & Liao, Y. (2018). Online adaptive optimum coordination of overcurrent relays. In *SoutheastCon 2018* (pp. 1–6).
24. Mishra, P., Pradhan, A. K., & Bajpai, P. (2018). Adaptive relay setting for protection of distribution system with solar PV. In *2018 20th National power systems conference NPSC* (pp. 1–5).
25. Shih, M. Y., Conde, A., Leonowicz, Z., & Martirano, L. (2017). An adaptive overcurrent coordination scheme to improve relay sensitivity and overcome drawbacks due to distributed generation in smart grids. *IEEE Transactions on Industry Applications, 53*(6), 5217–5228.
26. Naveen, P., & Jena, P. (2020). Adaptive protection scheme for microgrid with multiple point of common couplings. *IEEE Systems Journal, 15*(4), 5618–5629.
27. Muda, H., & Jena, P. (2017). Sequence currents based adaptive protection approach for DNs with distributed energy resources. *IET Generation, Transmission & Distribution, 11*(1), 154–165.

28. El-Hamrawy, A. H., Ebrahiem, A. A. M., & Megahed, A. I. (2022). Improved adaptive protection scheme based combined centralized/decentralized communications for power systems equipped with distributed generation. IEEE Access.
29. Momesso, A. E., Bernardes, W. M. S., & Asada, E. N. (2020). Adaptive directional overcurrent protection considering stability constraint. *Electric Power Systems Research, 181*, 106190.
30. Ghadiri, S. M. E., & Mazlumi, K. (2020). Adaptive protection scheme for microgrids based on SOM clustering technique. *Applied Soft Computing, 88*, 106062.
31. Muda, H., & Jena, P. (2016). Superimposed adaptive sequence current based microgrid protection: A new technique. *IEEE Transactions on Power Delivery, 32*(2), 757–767.
32. Tambun, R. C. S., Banjar-Nahor, K. M., Hariyanto, N., Rahman, F. S., & Rahmani, R. (2021). Adaptive protection coordination scheme for distribution system under penetration of distributed generation. In *2021 3rd International conference on high voltage engineering and power systems ICHVEPS* (pp. 355–360).
33. Nsengiyumva, E., Saulo, M. J., & Nyakoe, G. N. (2018). Adaptive protection scheme in distribution networks considering intermittency of DG using fuzzy logic controller. *International Journal of Engineering Research and Technology, 11*(7), 1179–1198.
34. Wadie, F., Abdulgawad, E., & Abd-Allah, A. M. (2023). Adaptive real-time protection scheme for distribution networks with high penetration levels of renewable energy resources. *Ain Shams Engineering Journal, 14*(7), 102005.
35. Song, Y., Xuan, Q., & Johns, A. (1997). Protection scheme for EHV transmission systems with thyristor controlled series compensation using radial basis function neural networks. *Electric Machines and Power Systems, 25*(5), 553–565.
36. Uma, U., Ekwue, A., & Ejiogu, E. (2021). Adaptive distance protection scheme for mutually coupled line. *Journal of Electrical Engineering & Technology, 16*(1), 131–140.
37. Zayandehroodi, H., Mohamed, A., Farhoodnea, M., & Mohammadjafari, M. (2013). An optimal radial basis function neural network for fault location in a distribution network with high penetration of DG units. *Measurement, 46*(9), 3319–3327.
38. Zayandehroodi, H., Mohamed, A., Shareef, H., & Mohammadjafari, M. (2010). A new protection scheme for distribution network with distributed generations using radial basis function neural network. *International Journal of Emerging Electric Power Systems, 11*, 5.
39. Rockefeller, G., Wagner, C., Linders, J., Hicks, K., & Rizy, D. (1988). Adaptive transmission relaying concepts for improved performance. *IEEE Transactions on Power Delivery, 3*(4), 1446–1458.
40. Misbahuddin, S. (2010). Fault tolerant remote terminal units RTUs in SCADA systems. In *2010 International symposium on collaborative technologies and systems* (pp. 440–446).
41. Atwa, Y., El-Saadany, E., Salama, M., & Seethapathy, R. (2009). Optimal renewable resources mix for distribution system energy loss minimization. *IEEE Transactions on Power Systems, 25*(1), 360–370.
42. Hung, D., Mithulananthan, N., & Bansal, R. (2010). Analytical expressions for DG allocation in primary distribution networks. *IEEE Transactions on Energy Conversion, 25*(3), 814–820.
43. Acharya, N., Mahat, P., & Mithulananthan, N. (2006). An analytical approach for DG allocation in primary distribution network. *International Journal of Electrical Power & Energy Systems, 28*(10), 669–678.
44. Duong, T. L., Nguyen, P. T., Vo, N. D., & Le, M. P. (2021). A newly effective method to maximize power loss reduction in distribution networks with highly penetrated distributed generations. *Ain Shams Engineering Journal, 12*(2), 1787–1808.
45. Abdelhamid, M., Kamel, S., Korashy, A., Tostado-Veliz, M., Banakhr, F. A., & Mosaad, M. I. (2021). An adaptive protection scheme for coordination of distance and directional overcurrent relays in distribution systems based on a modified school-based optimizer. *Electronics, 10*(21), 2628.
46. Al-Anbarri, K., & Majeed, W. (2012). A reliable load flow method for radial distribution systems. *J Eng Dev, 16*, 2.
47. Phadke, A., & Thorp, J. (2009). *Computer relaying for power systems*. Wiley.
48. Venkatesh, B., Ranjan, R., & Gooi, H. (2004). Optimal reconfiguration of radial distribution systems to maximize loadability. *IEEE Transactions on Power Systems, 19*(1), 260–266.
49. Mahesh, K., Nallagownden, P. A., & Elamvazuthi, I. A. (2015). Optimal placement and sizing of DG in distribution system using accelerated PSO for power loss minimization. In: *2015 IEEE conference on energy conversion (CENCON)* (pp. 193–198). IEEE.